ARTICLE

Polarization and Local Reactivity on Organic Ferroelectric Surfaces: Ferroelectric Nanolithography Using Poly(vinylidene fluoride)

Christopher Rankin,* Chun-Han Chou, David Conklin, and Dawn A. Bonnell

Materials Science and Engineering, University of Pennsylvania, Philadelphia, Pennsylvania 19104

ABSTRACT Molecular polarization of ferroelectric poly(vinylidene fluoride) (PVDF) is manipulated at the nanometer scale in order to influence the local electronic structure and reactivity at the surface. A direct current voltage, applied through a conductive scanning probe tip, is used to pattern ferroelectric domains in a PVDF thin film, and the polarization direction of these domains influences the kinetics of electron exchange at the surface. By means of a surface photoreduction reaction, which occurs in a metal ion solution under ultraviolet irradiation, metal nanoparticles are deposited in predetermined configurations on polymer surfaces. The photoexcited carriers are generated from defect states within the energy gap of the material, and these gap states are found not only at the interface but throughout the bulk polymer. This represents the first demonstration of ferroelectric nanolithography on an organic substrate and opens the door to applications in organic electronics.

KEYWORDS: nanofabrication · directed assembly · patterning · electo-optic properties · PVDF · poly(vinylidene fluoride) · ferroelectric

Recent advances in nanomaterials synthesis have yielded an ever-increasing array of functional components from which to assemble devices ranging from molecular electronics to chemical sensors. The ultimate goal in exploiting the new nanomaterials is to assemble multiple components of diverse materials types into complex configurations. Ferroelectric nanolithography achieves this by controlling local electronic structure on oxide substrates that influences electron transfer at the surface.[1,2] The consequence is domain-specific chemical attachment on prepatterned surfaces. This versatile technique allows fabrication of device structures consisting of metal and/or oxide nanoparticles, functionalized organic molecules, and dielectric materials. Details of electron-polarization interactions and local patterning have been discussed in earlier reports.[3,4] Until now, the approach has been limited to oxide substrate materials such as lead zirconate titanate (PZT) and barium titanate. Achieving the same lithographic process on organic substrates would enable integration into new classes of applications, such as flexible electronics. Here we demonstrate nanoscale patterning on organic ferroelectric thin films, specifically poly(vinylidene fluoride) (PVDF), determine the origin of photoconduction in this compound, and combine these two processes to deposit metal nanoparticles *via* domain-specific photoreduction.

PVDF has been widely used for its ferroelectric, piezoelectric, and pyroelectric properties in a variety of applications including electro-acoustic transducers, ultrasonic diagnostic equipment, and ultrasonic hydrophones.[5] The permanent electrical polarization present in the ferroelectric β-phase of PVDF is due to the influence of highly electronegative fluorine on the polymer chain. The β-phase consists of parallel packing of trans chains, which fit into an orthorhombic unit cell.[6,7] The lattice is characterized by the point symmetry group C_{2v}, with lattice parameters $a = 8.58$ Å, $b = 4.91$ Å, and $c = 2.56$ Å.[8] The chain units, CH_2–CF_2, deviate from a perfect planar zigzag plane by an angle of approximately 7° due to steric hindrance.[8] There is a spontaneous alignment of the CF_2, which results in a permanent remnant polarization.

For this study, ~1 wt % PVDF (Dupont, Kynar) was dissolved in acetone and subsequently deposited by spin-coating at 3000 RPMS on (100) silicon coated with a 10 nm evaporated layer of gold. Spin-coating of PVDF was followed by an annealing treatment in a differential scanning calorimeter in order to control the cooling rate. The film morphology was found to depend on processing conditions. To produce optimum and consistent film structures, annealing temperatures were varied from 100 to 180

*Address correspondence to crankin@seas.upenn.edu.

Received for review June 24, 2007 and accepted October 02, 2007.

Published online October 12, 2007. 10.1021/nn7000728 CCC: $37.00

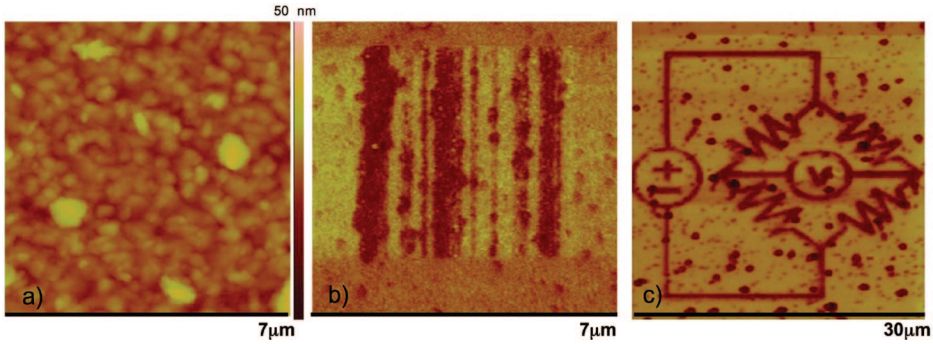

Figure 1. Topographic structure of a 50 nm thick PVDF film, revealing the flat but granular structure of the surface (a). Surface potential images of patterns poled on the PVDF surface, showing variation in feature size (b) and complexity in patterning (c).

°C, and cooling rates were varied from 20 to 0.1 °C/min. Annealing for 1 h at 180 °C and a cooling rate of 20 °C/min result in films exhibiting topographic features with ~50 nm lateral and 2 nm root-mean-square (rms) roughness. Comparisons were made of films deposited with and without the thin gold layer. The gold increases wetting and adhesion of the PVDF and provides a bottom electrode for poling and photoconductivity measurements. Domain patterning of the films was performed using a commercial atomic force microscope (AFM, Veeco, Dimension 3100) by applying a direct current (dc) voltage to a Pt/Ir-coated silicon scanning probe tip as it scanned in contact with the film. To ensure that ferroelectric domains have sufficient time for reorientation during patterning, the AFM tip was scanned at a relatively modest rate of 0.7 Hz. Scanning surface potential microscopy,[3] often referred to as Kelvin probe microscopy, was employed to characterize the patterned domains. A quantitative interpretation of potential images of ferroelectric surfaces is complicated by the interplay of atomic polarization and compensation charges; however, mapping the domain orientation is straightforward using this technique.[3] Photoconductivity was quantified from current–voltage (*I*/*V*) curves obtained in the presence and in the absence of ultraviolet (UV) radiation with a Pt/Ir-coated AFM tip as a top electrode and in a lateral two-point probe configuration. In both cases, the light was introduced *via* a fiber-optic cable perpendicular to the sample surface, irradiating an area of approximately 1 mm^2.

For 50 nm thick films, ±8 V on the tip, corresponding to applied electric fields of ±0.16 GV/m, produced positively and negatively oriented domains, respectively. This field, which is above the coercive field reported for solvent-formed PVDF films,[10] resulted in ferroelectric domain reorientation (Figure 1). Domains as large as 10 μm and as small as 70 nm were routinely produced. As shown in Figure 1, complete spatial control over domain orientation is achieved on the organic substrate, demonstrating its potential as a lithographic process. The feature size here does not represent a fundamental limit in domain stability. In ferroelectric polymers, the mechanism of polarization switching is the rotation of individual chains, and this rotation occurs by the propagation of kinks along the chain.[11] A smaller diameter AFM tip and short voltage pulses applied instead of a dc electric field would reduce the volume for electrically activated nucleation[10] and result in even smaller feature sizes. Similarly, domain patterning has been demonstrated with e-beam lithography and microelectrode stamping and is amenable to scale-up for applications.

The operational principle of ferroelectric nanolithography relies on the fact that electron/hole pairs created by optical absorption separate in the local electric field of ferroelectric domains; therefore, the mechanism of photoconductivity in the PVDF films must be determined. The photoconductance of a 50 nm PDVF film, determined with the AFM top electrode, is shown in

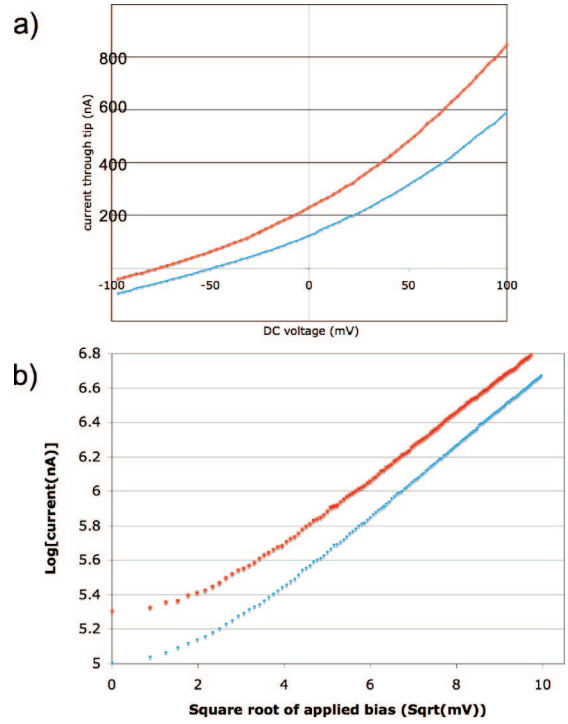

Figure 2. Linear (a) and logarithmic (b) comparisons of photoconductance measured with a SFM tip top electrode. UV radiation causes a 35% increase in current, and the linearity of (b) suggests that a Poole–Frenkel or Richardson–Schottky transport mechanism operates. Top curves represent current as a function of voltage with light ON, bottom with light OFF.

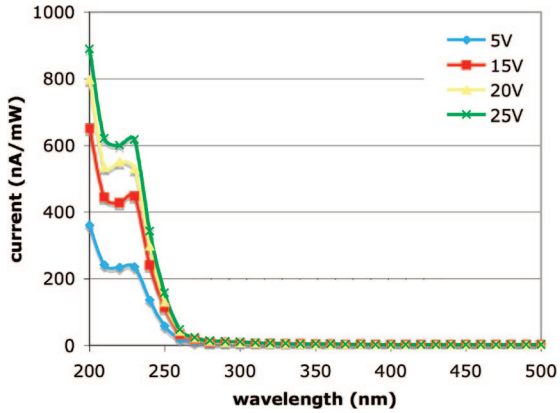

Figure 3. UV-stimulated photocurrent normalized by the power of the light source from a two-point probe configuration. The total current increase due to optical absorption is almost 2 orders of magnitude.

Figure 2. To eliminate potential ambiguity due to instrumental and sample-based artifacts, a control measurement was done first. The conductance of Si was measured in the same configuration and found not to increase with irradiation, demonstrating that the neither the Si substrate and AFM tip nor the detection instrumentation contributed to the photocurrent signal. As previously reported,[5,13] the carrier concentration increases under UV irradiation. While a capacitive current offsets the *I*/*V* curves at 0, the increase in conductance upon illumination is clear and on the order of 35% at 100 mV in this measurement. The apparent rectification in the data is likely due to the asymmetry in the fields from the electrodes, one a point source and the other a plane. The magnitude of the photocurrent is almost certainly affected by the geometry of illumination, which exposes a relatively large area and casts a shadow below the tip in the region of measurement. Nevertheless, optical absorption clearly occurs.

The band structure and density of states[14] of PVDF indicate that it is an insulator with a HOMO–LUMO gap of 6 eV. In an ideal PDVF film, carriers are not created at energies less than 6 eV. In contrast to inorganic crystals, organic crystals and polycrystals in particular contain a large density of defects such as chain conformational defects, dopants, and localized amorphous regions.[15–17] These defects are considered the source of the dc conductivity and the observed dark current. The energy levels and indeed the atomic structures of these defects are not known *a priori* but may be experimentally probed with the optical wavelength dependence of conductance. Figure 3 shows conductance spectra from the two-point probe configuration. Above 250 nm (below 5 eV), there is no effect of illumination on conductance over the applied bias range range of 5–30 V. Between 250 and 200 nm (5 and 6.2 eV), the conductance changes by more than 2 orders of magnitude. There is a significant increase beginning about 1.5 eV below the lowest unoccupied orbital and a large increase in charge carrier generation at the band gap energy, as expected. Optical measurements on conjugated and fluorinated polymers offer some insight on these energy levels. The polystyrene $\pi-\pi^*$ transition occurs in exactly this energy range, and chain ends and defects shift the absorption to lower energies. Similarly, polymers of alternating segments of CF_2 and CH_2 exhibit a reduction in energy gap with irregularities in the chain sequence.[22] Defects or structural inhomogeneity can have pronounced effects on the electrical and optical properties of this class of organic compounds.[22,23] In comparison to these compounds with similar bonding characteristics, it is reasonable to attribute the absorption between 5 and 6 eV to optically active defects.

Several mechanisms have been proposed for conduction in insulating polymers. The goal here is not to isolate the hopping mechanism but rather to determine the origin of the photocarriers. Nevertheless, general aspects of the conduction mechanism are apparent from the data. The functional relationship in Figure 2 excludes ohmic hopping and space-charge-limited con-

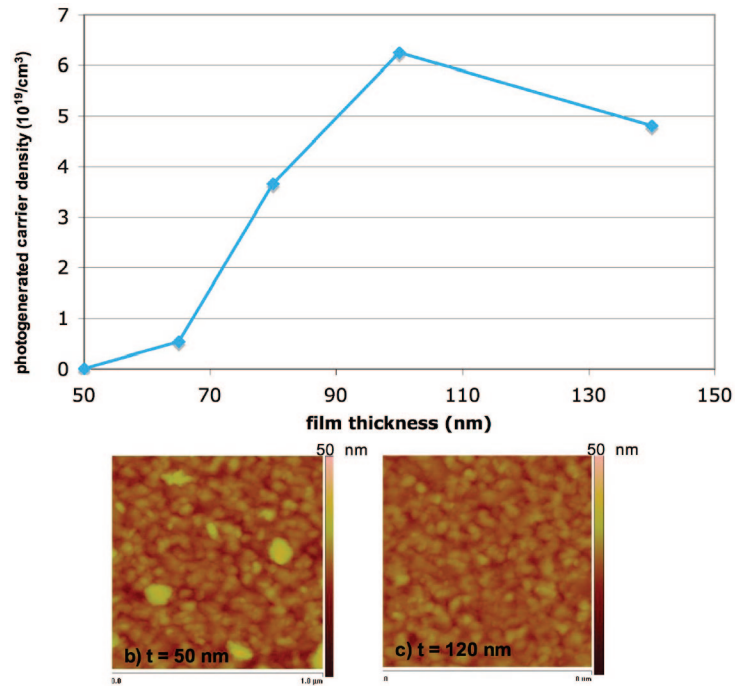

Figure 4. Poole–Frenkel conduction from bulk defects. (a) Photocarrier density as a function of film thickness, showing increasing photocarrier density with increasing film thickness; each data point was calculated by averaging over 10 *I*/*V* curves. (b,c) Tapping mode scanning probe images of PVDF film morphology, revealing no appreciable change in grain size and film morphology across the relevant thickness range.

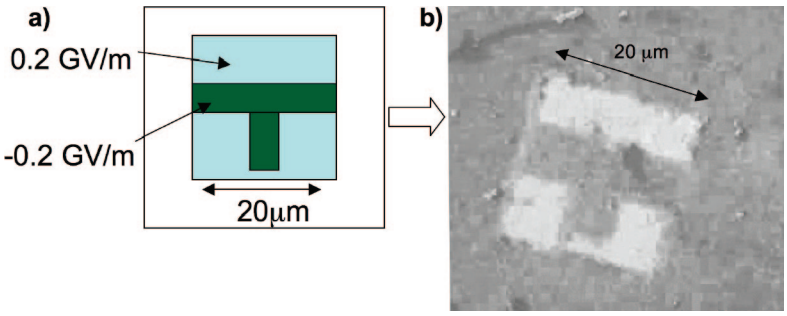

Figure 5. Ferroelectric nanolithography on PVDF. (a) Schematic of the poling pattern applied to 50 nm PVDF film. (b) Optical microscopy image, showing heavy silver metal deposition on the region of negative applied dc voltage and little silver coverage on oppositely polarized regions, demonstrating the domain-specific reactivity resulting from the ferroelectric and photoconductive behavior of PVDF.

duction as potential mechanisms. The nearly linear relationship, shown in Figure 2b, suggests that the mechanism is either Richardson–Schottky or Poole–Frenkel conduction. The Richardson–Schottky mechanism arises out of the interaction between the electrode and polymer, while the Poole–Frenkel phenomenon is considered a bulk effect.[18] Both mechanisms yield the following current function:

$$I = A \exp(\frac{1}{2}\beta V^{1/2} - \varphi_0)/kT \quad (1)$$

For the Richardson–Schottky interface mechanism, $\beta = (e^3/\pi\epsilon\epsilon_0 d)^{1/2}$, φ_0 is the energy barrier height at the interface, e is the unit charge of an electron, d is the insulator thickness, ϵ is the dielectric constant of the insulating polymer, and ϵ_0 is the permittivity of free space. For the Poole–Frenkel bulk mechanism, φ_1 represents the difference in energy between a trap state in the insulator and the conduction band energy. From β, which is calculated from the slope in Figure 2b, the dielectric constant can be estimated and is found to be ~1.8. Although this value is lower than what is typically reported for PVDF,[24] our estimation is valid to within an order of magnitude.

Controversy exists regarding the origin of photoconductivity in bulk PVDF. Sasabe *et al.*[5] refer to surface carriers moving in the internal electric field resulting from the remnant polarization. Ogden and Gookin observed a bulk photovoltaic response.[13] Micheron[19] attributed the photocurrent to either electrode photoinjection or surface-state photoexcitation. In order to determine if the photocurrent in the thin-film PVDF is due to surface or bulk processes, the film thickness dependence of carrier concentration was determined as N_c(carriers/cm^3) $= t/RAe\mu_N$ by averaging over 10 I/V curves for each film thickness, where t is the film thickness, R is the resistance, A is the electrode area, e is the elementary charge of an electron, and μ_N is the carrier mobility, taken to be 2×10^{-8} cm^2 V^{-1} s^{-1}, as reported earlier.[20] The monotonic increase in photocarrier concentration with increasing film thickness to 100 nm, shown in Figure 4, demonstrates that the photogenerated electrons do not arise exclusively from the interface or surface but must be generated throughout the bulk of the film. Furthermore, the increase in photocarrier concentration is not a consequence of morphological changes, as the topographic structures compared in Figure 4b,c reveal negligible variation in crystallite size or surface roughness. As the film thickness approaches the absorption depth, the photocarrier concentration saturates. These results imply that bulk defects are primarily, or at least significantly, responsible for absorption sites that produce electron/hole pairs.

The polarization dependence of the photocurrent resulting from these defects was exploited to deposit silver nanoparticles in a predetermined pattern on the polymer surface. Patterning was performed on a 50 nm thick PVDF film by reduction of a 10^{-3} M $AgNO_3$ solution under UV irradiation for 20 min. Figure 5 shows the geometric pattern used to pole the surface and the resulting pattern of Ag nanoparticle deposition. The darker contrast in the optical image corresponds to regions covered with nanoparticles, while the brighter contrast regions contain few particles. In heavily deposited patterns, the Ag nanoparticles range from 50 to 200 nm and aggregate into clusters. The solution concentration and reaction time can be used to vary the deposit morphology. The conditions of domain-specific photodeposition on PVDF are similar to those of oxide substrates, on which a wide range of nanostructures can be patterned. Future studies will expand the range of nanostructures that can be lithographically patterned on organic substrates.

In summary, the orientation of ferroelectric domains in PVDF thin films was controlled at the nanoscale using local electrodes, and domain-specific reactivity was demonstrated. Combined with domain patterning, this domain-specific reactivity enables deposition of nanoparticles in complex configurations on the film surface. These results demonstrate that the ferroelectric polymer PVDF can be utilized as a flexible template for the directed assembly of metal nanostructures and can, in principle, be functionalized further with electronically or optically active molecules, providing a backbone for the assembly of nanodevices.

METHODS

To prepare the PVDF films, 1 wt % PVDF (Dupont, Kynar) was dissolved in acetone (HPLC grade, Sigma-Aldrich) and subsequently spin-coated on gold-coated Si(100) with the native oxide intact. The gold coating, with a thickness of 10 nm, was applied to the silicon surface by evaporation using a commercial evaporator (Thermionics Vacuum Products model VE-90). Film heat treatment was performed using a commercial differential scanning calorimeter (TA Instruments model 2920). Topographical investigation as well as patterning of ferroelectric domains was accomplished using a commercial atomic force microscope (Veeco Dimension 3100) with Pt/Ir-coated silicon AFM tips (nanosensors, spring constant = 3 N/m). Broad illumination was provided by a 200 W Hg arc lamp (Oriel, model 68811) before filtering with a commercial monochromator (Newport, model 74000). Two-point electrical measurements were conducted in a LakeShore Desert Cryogenics TTP6 probe station using a Keithley electrometer (model 6517A).

Acknowledgment. This research was partially supported by the Nano/Bio Interface Center through the National Science Foundation NSEC DMR-0425780 and partially supported by the the National Science Foundation IGERT DGE02-21664. Facilities of the MRSEC are gratefully acknowledged. We also thank Maxim Nikiforov for valuable discussion and assistance with figures.

REFERENCES AND NOTES

1. Lei, X.; Li, D.; Shao, R.; Bonnell, D. A. In situ Deposition/positioning of Magnetic Nanoparticles with Ferroelectric Nanolithography. *J. Mater. Res.* **2005**, *20*, 712–718.
2. Kalinin, S. V.; Bonnell, D. A.; Alvarez, T.; Lei, X.; Hu, Z.; Ferris, J. H. Polarization and Local Reactivity on Ferroelectric Surfaces: A New Route to Complex Nanostructures. *Nano Lett.* **2002**, *2*, 589–593.
3. Kalinin, S. V.; Bonnell, D. A. Local Potential and Polarization Screening on Ferroelectric Surfaces. *Phys. Rev. B* **2001**, *63*, 125411.
4. Kalinin, S. V.; Bonnell, D. A.; Alvarez, T.; Lei, X.; Hu, Z.; Shao, R.; Ferris, J. H. Ferroelectric Lithography of Multicomponent Nanostructure. *Adv. Mater.* **2004**, *16*, 795–799.
5. Sasabe, H.; Nakayama, T.; Kumazawa, K.; Miyata, S.; Fukada, E. Photovoltaic Effect in Poly(vinylidene fluoride). *Polym. J.* **1981**, *13*, 967–973.
6. Nakamura, K.; Sawai, D.; Watanabe, Y.; Taguchi, D.; Takahashi, Y.; Furukawa, T.; Kanamoto, T. Effect of Annealing on the Structure and Properties of Poly(vinylidene fluoride) Beta-form films. *J. Polym. Sci. B: Polym. Phys.* **2003**, *41*, 1701.
7. Lu, F.; Hsu, S. L. Spectroscopic Study of the Electric Field Induced Microstructural Changes in Poly(Vinylidene) Fluoride. *Polymer* **1984**, *25*, 1250.
8. Kochervinskii, V. V. Piezoelectricity in Crystallizing Ferroelectric Polymers: Poly(vinylidene fluoride) and its Copolymers (A Review). *Crystallogr. Rep.* **2003**, *48*, 649–675.
9. Ohigashi, H. Electromechanical Properties of Polarized Polyvinylidene Fluoride Films as Studied by the Piezoelectric Resonance Method. *J. Appl. Phys.* **1976**, *47*, 949–955.
10. Vizdrik, G.; Ducharme, S.; Fridkin, V. M.; Yudin, S. G. Kinetics of Ferroelectric Switching in Ultrathin Films. *Phys. Rev. B* **2003**, *68*, 094113.
11. Dvey-Aharon, H.; Sluckin, T. J.; Taylor, P. L.; Hopfinger, A. J. Kink Propagation as a Model for Poling in Poly(vinylidene fluoride). *Phys. Rev. B* **1980**, *21*, 3700.
12. Nunes, J. S.; Sencadas, V.; Wu, A.; Vilarinho, P. M.; Lancero-Mendez, S. Electrical and Microstructural Changes of β-PVDF under Uniaxial Stress Studied by Scanning Force Microscopy. *Adv. Mater. Forum III* **2006**, *514*, 945–951.
13. Ogden, T. R.; Gookin, D. M. Bulk Photovoltaic Effect in Polyvinylidene Fluoride. *Appl. Phys. Lett.* **1984**, *45*, 995–997.
14. Duan, C. G.; Mei, W. N.; Hardy, J. R.; Ducharme, S.; Choi, J.; Dowben, P. A. Comparison of the Theoretical and Experimental Band Structure of Poly(Vinylidene Fluoride) Crystal. *Europhys. Lett.* **2003**, *61*, 81–87.
15. Bune, A.; Ducharme, S.; Fridkin, V.; Blinov, L.; Palto, S.; Petukhova, N.; Yudin, S. Novel Switching Phenomena in Ferroelectric Langmuir-Blodgett Films. *Appl. Phys. Lett.* **1995**, *67*, 3975–3977.
16. Bodhane, S. P.; Shirodkar, V. S. Space-Charge-Limited Conduction in Vacuum-Deposited PVDF films. *J. Appl. Polym. Sci.* **1999**, *74*, 1347–1354.
17. Sussman, A. Space-Charge-Limited Currents in Copper Phthalocyanine Thin Films. *J. Appl. Phys.* **1967**, *38*, 2738–2748.
18. Mead, C. A. Electron Transport Mechanisms in Thin Insulating Films. *Phys. Rev.* **1962**, *128*, 2088–2093.
19. Micheron, F. Comment on "Bulk Photovoltaic Effect in Polyvinylidene fluoride". *Appl. Phys. Lett.* **1985**, *47*, 67–68.
20. Gross, B.; Seggern, H.; Multhaupt, R. G. Carrier Mobilities in Poly(Vinylidene Fluoride). *J. Phys. D: Appl. Phys.* **1985**, *18*, 2497–2504.
21. Ye, Y.; Jiang, Y.; Wu, Z.; Zeng, H.; Yang, Y.; Li, W. Characterization and Ferroelectric Properties of Electric Poled PVDF Films. *Proceedings of the 12th International Symposium on Electrets*; IEEE: Piscataway, NJ, 2005.
22. French, R. H.; Wheland, R. C.; Qiu, W.; Lemon, M. F.; Zhang, E.; Gordon, J.; Petrov, V. A.; Cherstkov, V. F.; Delaygina, N. I. Novel Hydrofluorocarbon Polymers for use as Pellicles in 157 nm Semiconductor Photolithography: Fundamentals of Transparency. *J. Fluorine Chem.* **2003**, *122*, 63–80.
23. French, R. H.; Winey, K. I; Yang, M. K.; Qiu, W. Optical Properties and van der Waals-London Dispersion Interactions of Polystyrene Determined by Vacuum Ultraviolet Spectroscopy and Spectroscopic Ellipsometry. *Aust. J. Chem.* **2007**, *60*, 251–263.
24. Chiang, C. K.; Popielarz, R. Polymer Composites with High Dielectric Constant. *Ferroelectrics* **2002**, *275*, 1–9.